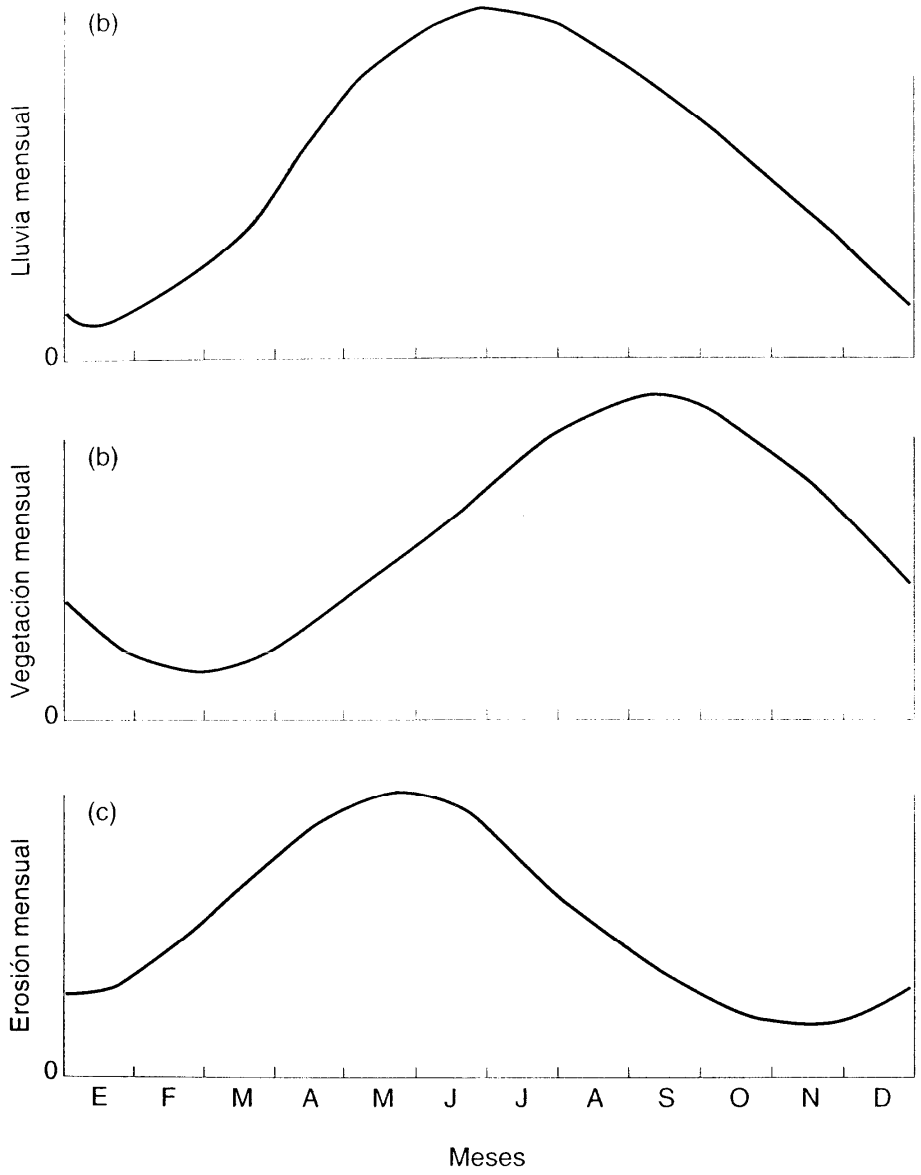


**Figura 1.3.** Ciclos estacionales de lluvia, cobertura vegetal y erosión en un clima subhúmedo (según Kirkby 1980a).

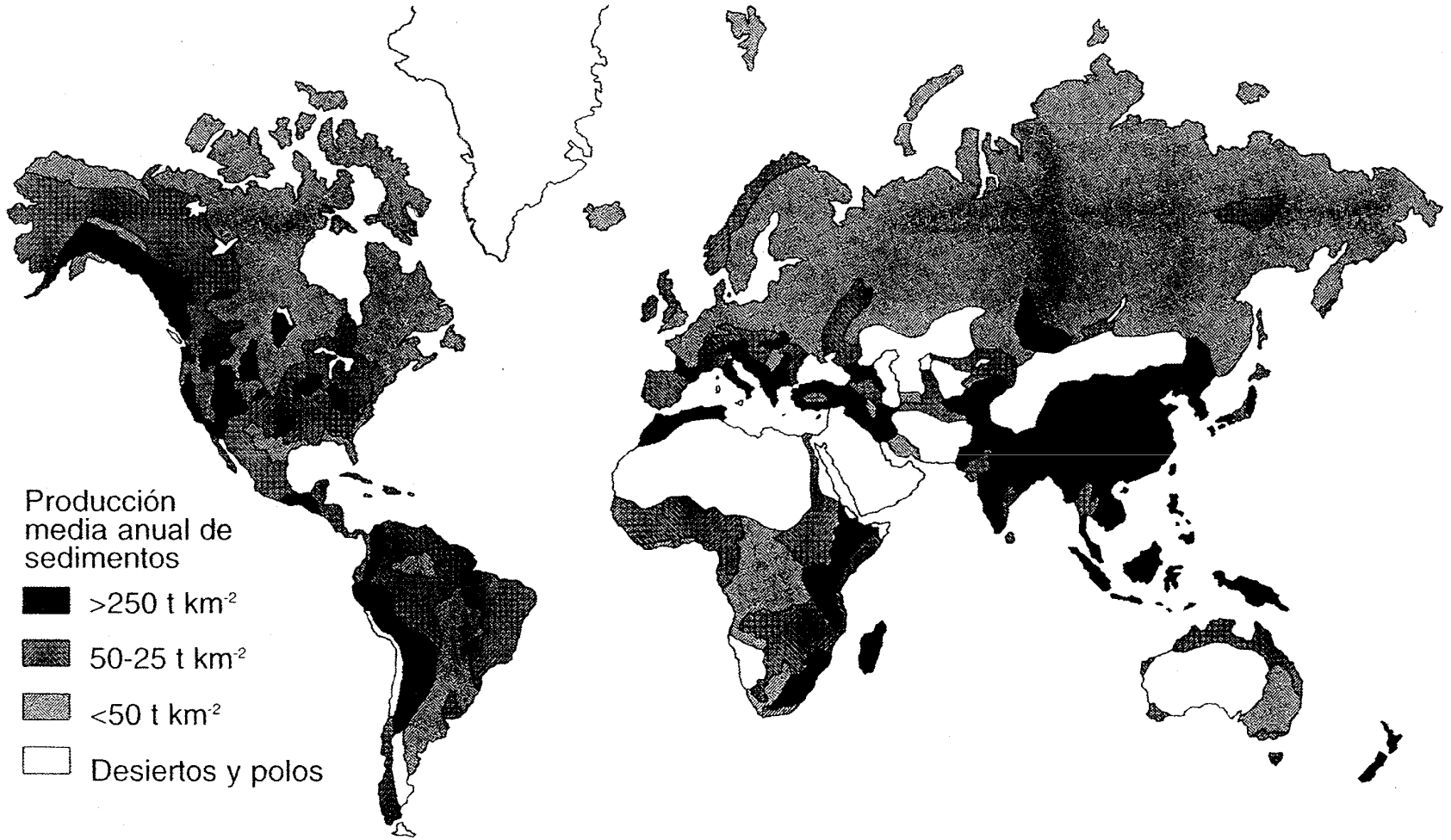


**Figura 1.2.** Un intento de representar a escala mundial las variaciones de sedimentos en suspensión (según Walling y Webb 1983).

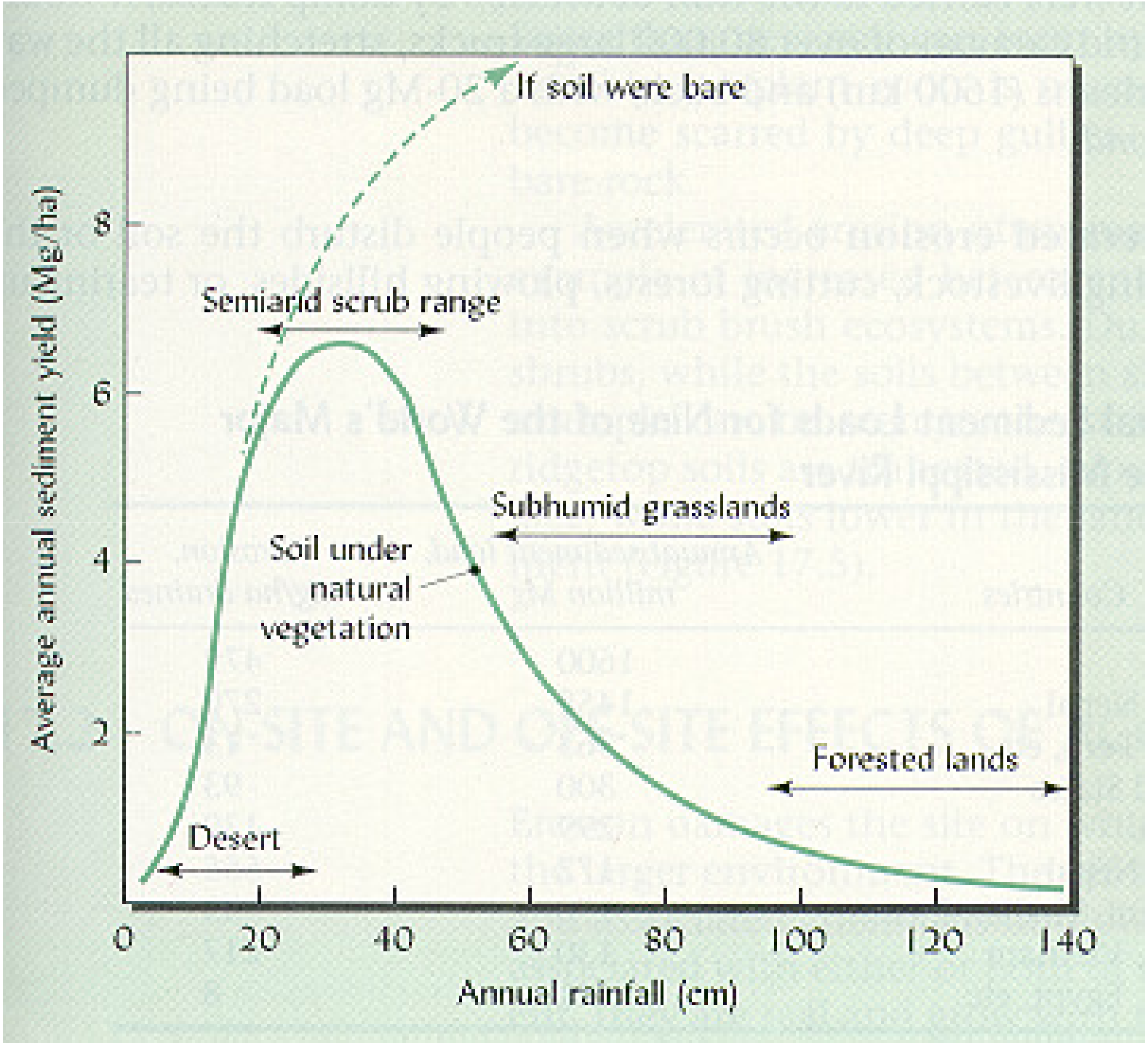
If soil were bare
Semiarid scrub range
Subhumid grasslands
Soil under
natural
vegetation
Forested lands
Desert
Average annual sediment yield (Mg/ha)
8
6
4
2
0
20
40
60
80
100
120
140
Annual rainfall (cm)

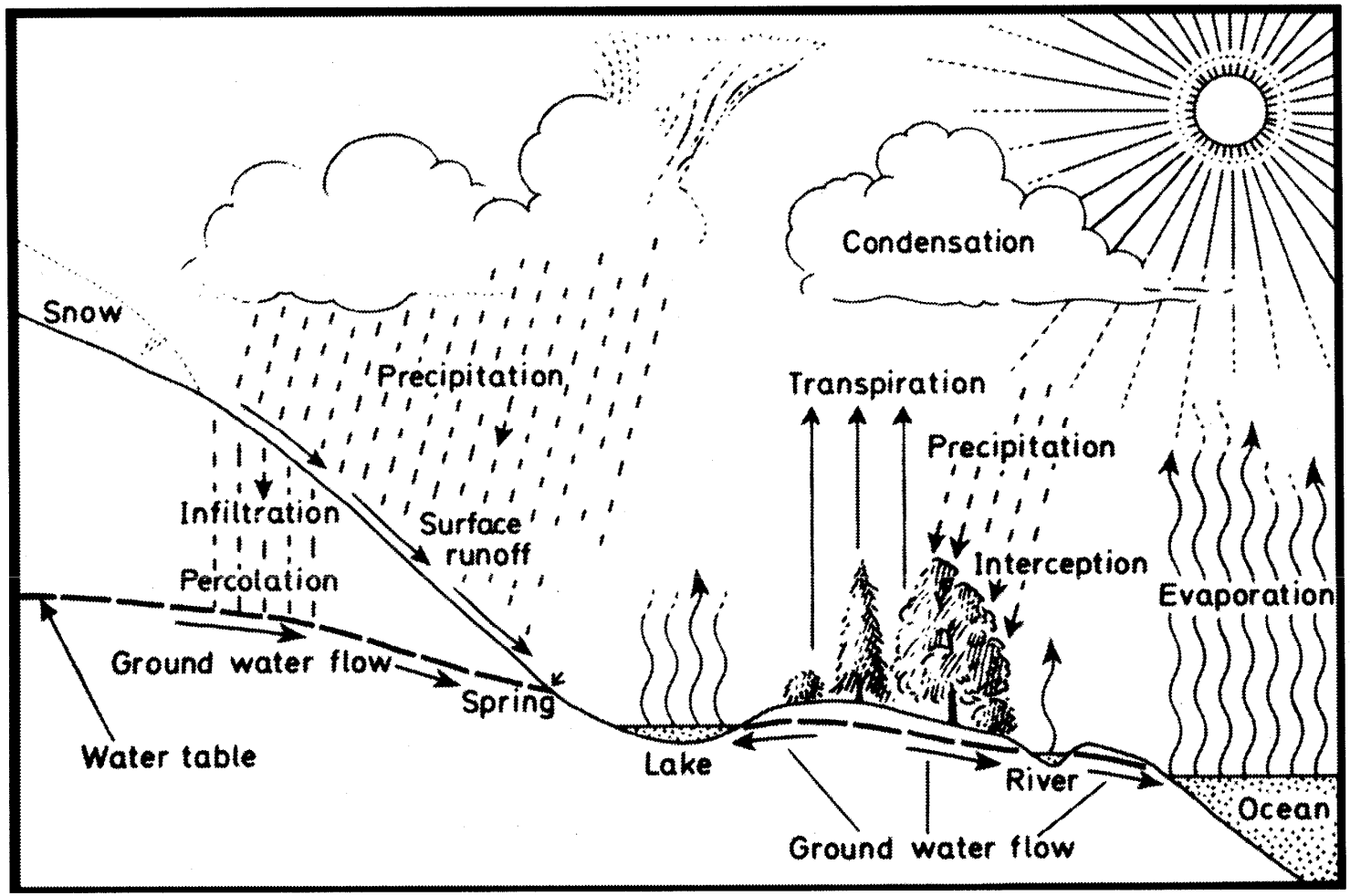


**FIGURE 1.1** The hydrologic cycle. (From Shaw, E. M., Hydrology—a multidisciplinary subject, in *Environment, Man and Economic Change,* Phillips, A. D. M. and Turton, B. J., Eds., Longman, London and New York, 1975, 164. ©Longman Group Limited 1975. With permission.)

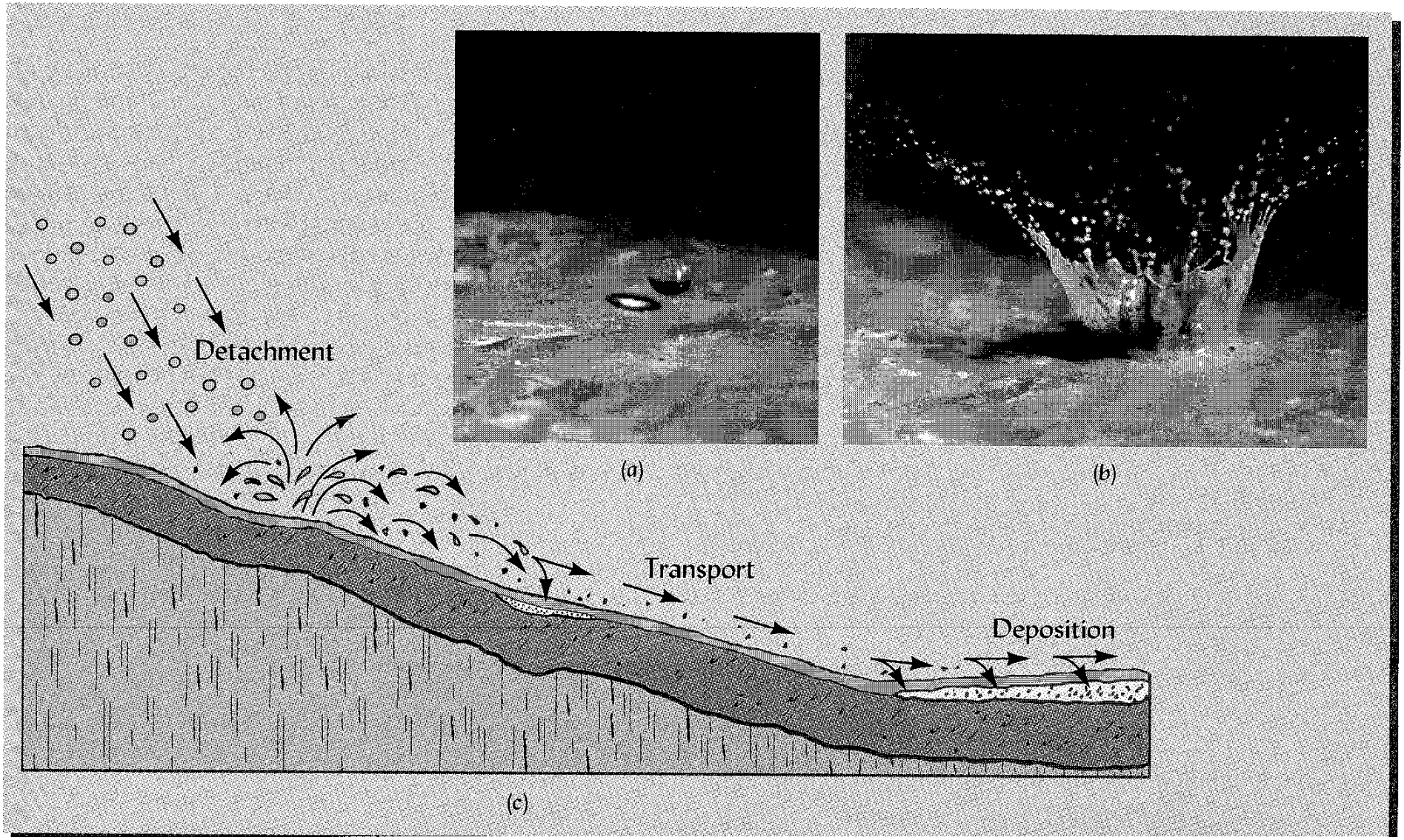
Detachment
Transport
Deposition
(a)
(b)
(c)

Desprendimento → Salpicamento

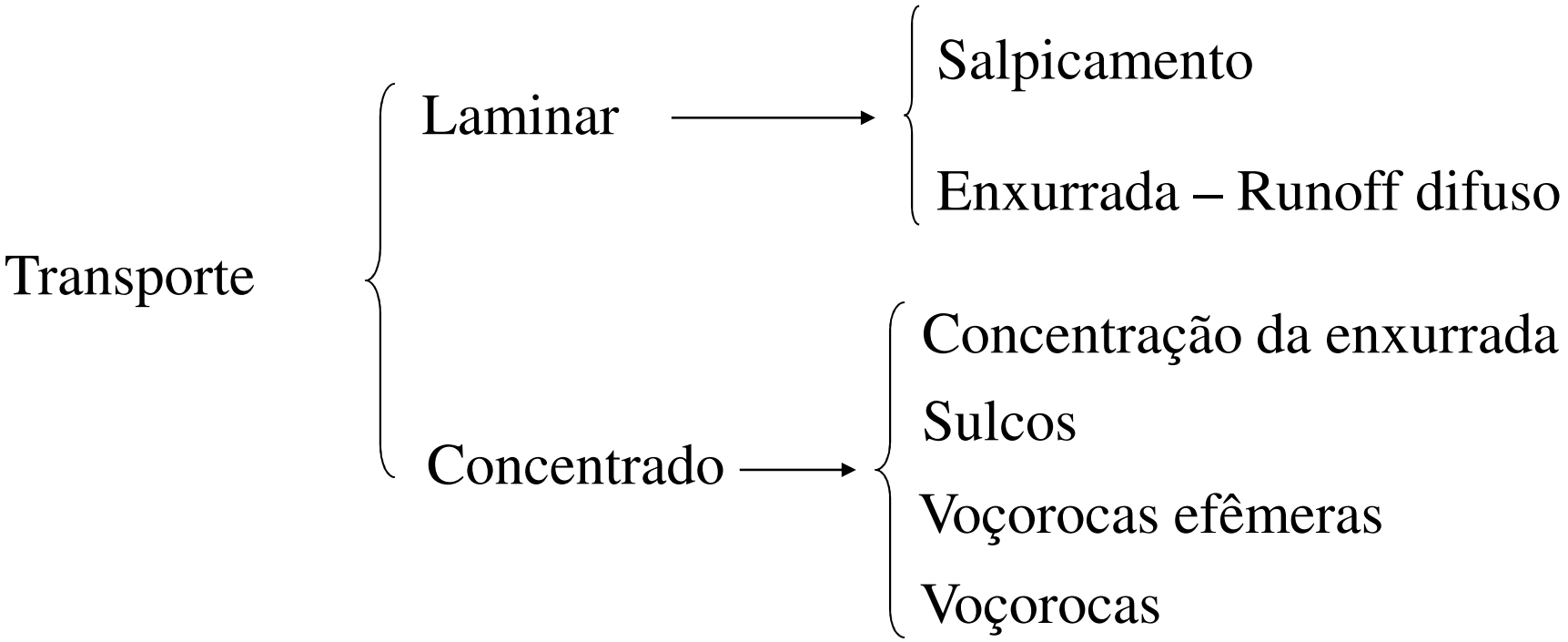

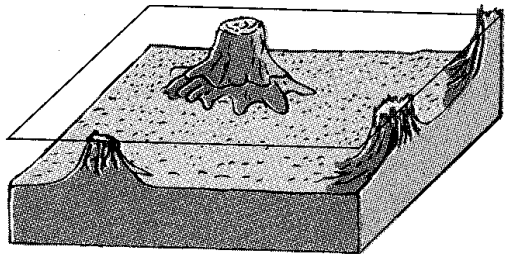

(*a*) Sheet erosion

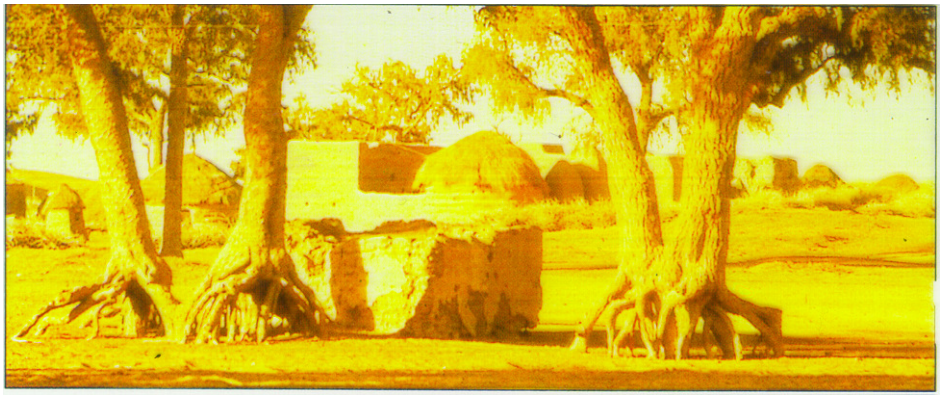

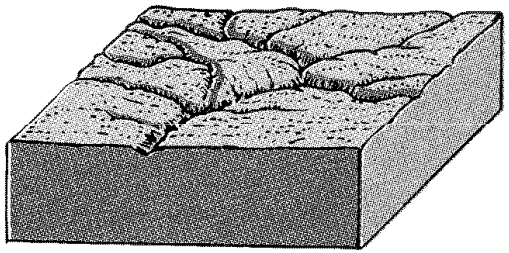

(*b*) Rill erosion

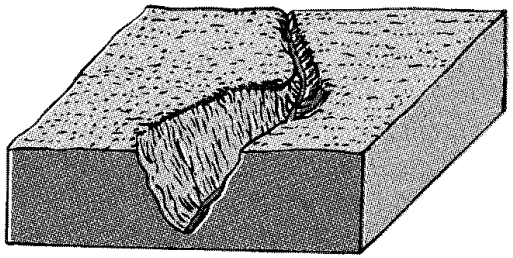

(*c*) Gully erosion

# Impacto da Gota de Chuva

- desprendem partículas de solo no local que sofre impacto;

- transportam, por salpicamento, as partículas desprendidas;

- imprimem energia, em forma de turbulência, à água superficial.

# Energia Cinética e Momento da Gota de Chuva

É muito importante conhecer a força com que a chuva impacta contra o solo.

A energia cinética e o momento são calculadas a partir da massa e da velocidade:

$$Ec = \frac{1}{2} mv^2 \qquad\qquad Mom = mv$$

Energia cinética da chuva e da enxurrada:

| | Chuva | Enxurrada |
|---|---|---|
| Massa | Suponha uma massa de queda da chuva = R | Suponha 25% de enxurrada, e a massa da enxurrada = R/4 |
| Velocidade | Suponha uma velocidade de 8m/s | Suponha a velocidade de escorrimento na superfície de 1m/s |
| Energia Cinética | 1/2 x R x $(8)^2$ = 32R | 1/2 x R/4 x $(1)^2$= R/8 |

Fonte: Hudson (1973)

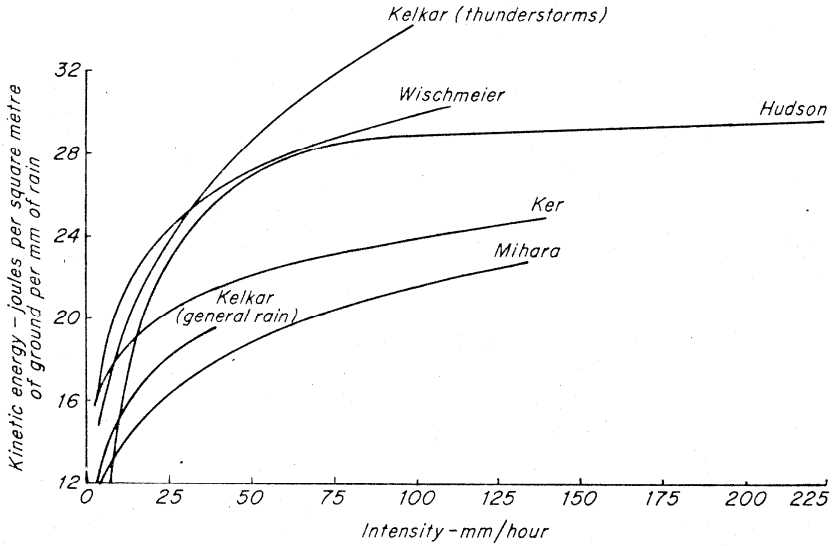


FIGURE 3.9 *The relation between kinetic energy of rainfall and intensity. Each curve extends to the highest intensity recorded. The studies were carried out in the following countries:* HUDSON—*Rhodesia,* KELKAR—*India,* KER—*Trinidad,* MIHARA—*Japan,* WISCHMEIER—*United States*

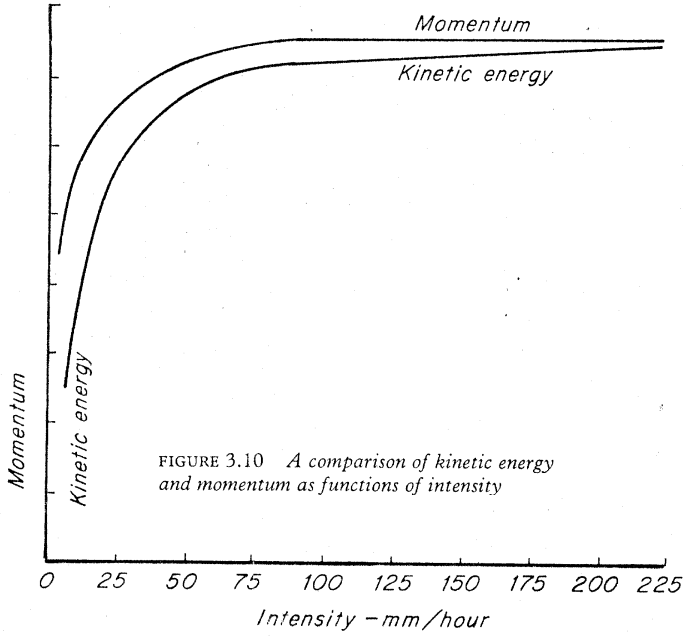


FIGURE 3.10 *A comparison of kinetic energy and momentum as functions of intensity*

# Tamanho e Velocidade Terminal da Gota de Chuva

| Diâmetro da gota de chuva | Velocidade Terminal | Altura da queda com a qual a gota de água adquire 95% da sua velocidade terminal |
|---|---|---|
| mm | m/s | m |
| 1 | 4,0 | 2,2 |
| 2 | 6,5 | 5,0 |
| 3 | 8,1 | 7,2 |
| 4 | 8,8 | 7,8 |
| 5 | 9,1 | 7,6 |
| 6 | 9,3 | 7,2 |

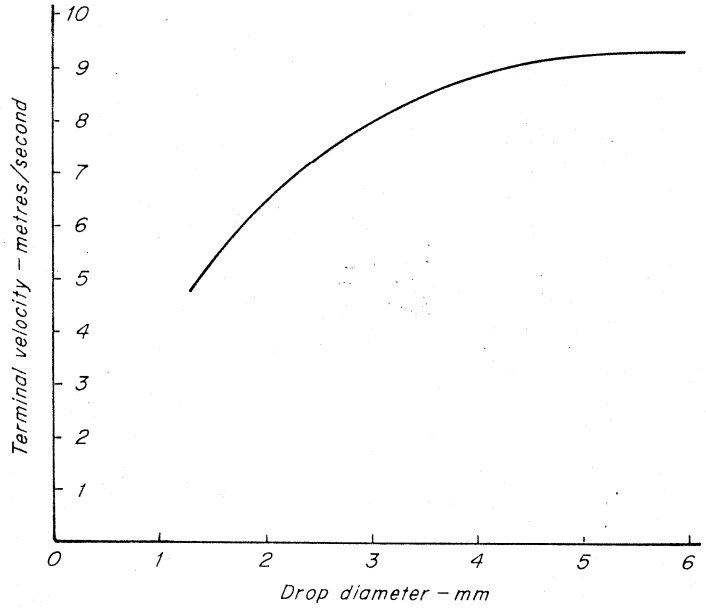


FIGURE 3.8 *The terminal velocity of raindrops* (data from LAWS 1941)

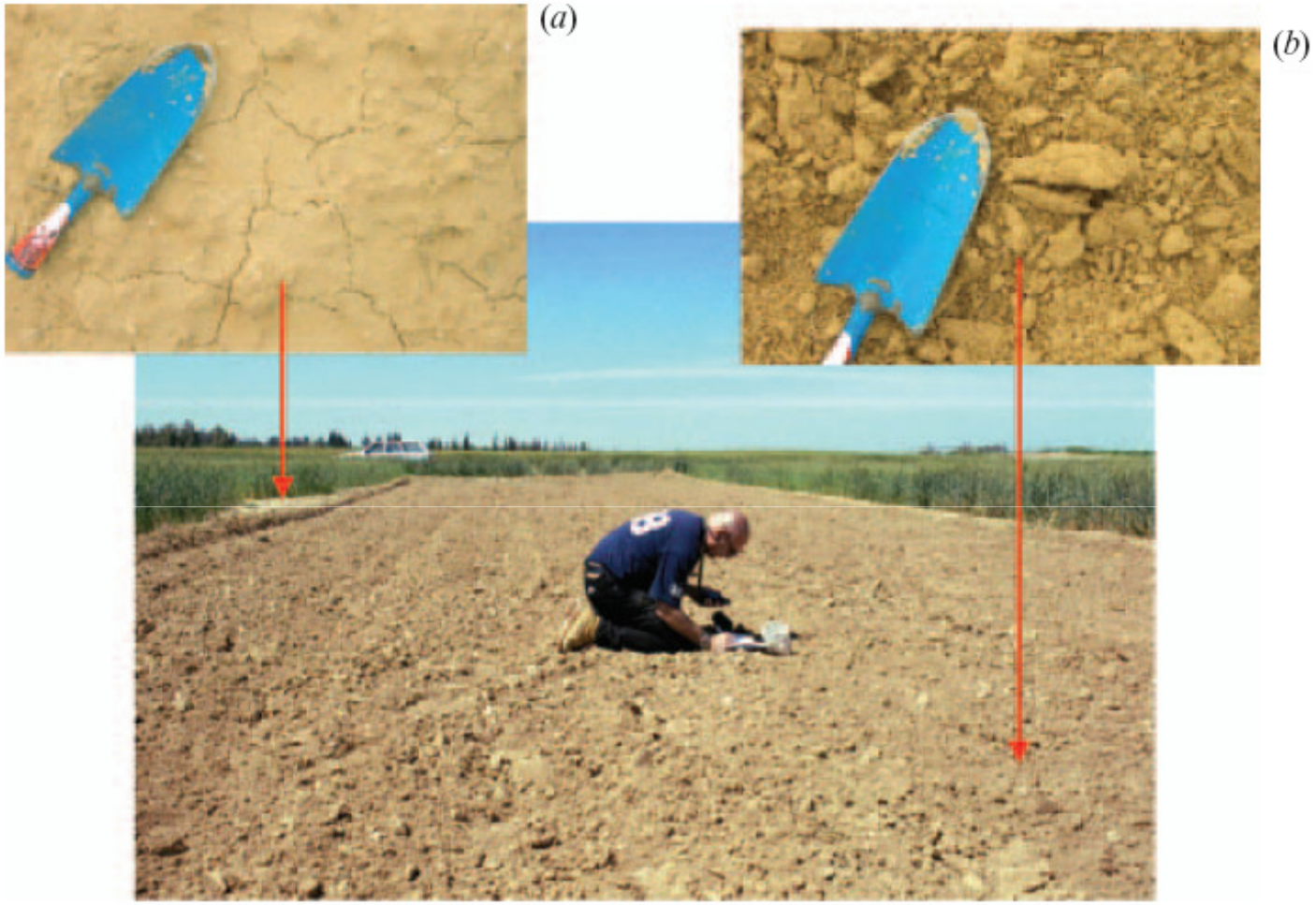


Figure 5. An overview of plot 3 (see figure 3(*b*)) in its discus (non-crust), and two enlarged images of the (*a*) crusted and (*b*) non-crusted soils from a distance of 80 cm.

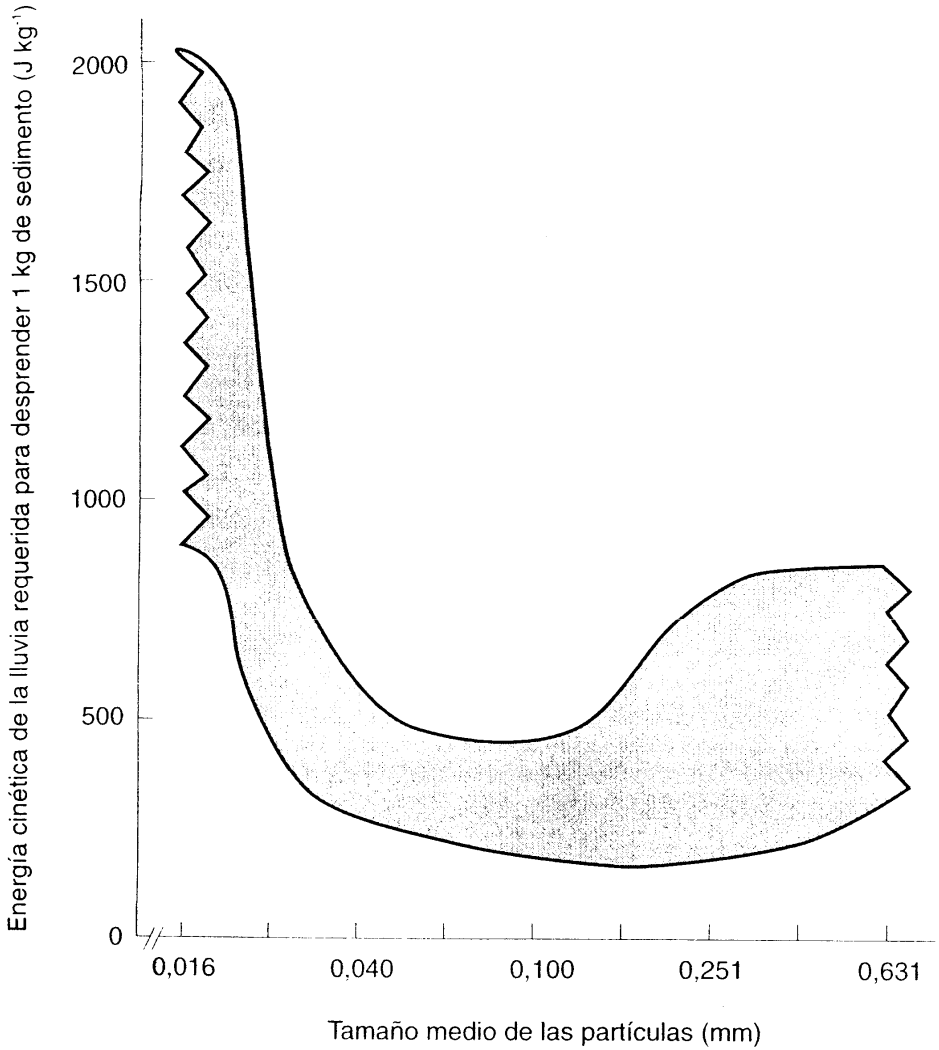


**Figura 2.2.** Relación entre el tamaño medio de las partículas del suelo y energía de la lluvia requerida para desprender 1 kg de sedimentos. El área sombreada muestra la variación de los resultados experimentales (según Poesen 1992).

# Raindrop impact phenomena: The rigid case

Impacto da gota no solo
- Compressão pelo impacto
- Cisalhamento pelo “lateral jetting of water”

Qual é a magnitude do impacto?

Quais são as velocidades do fluxo lateral?

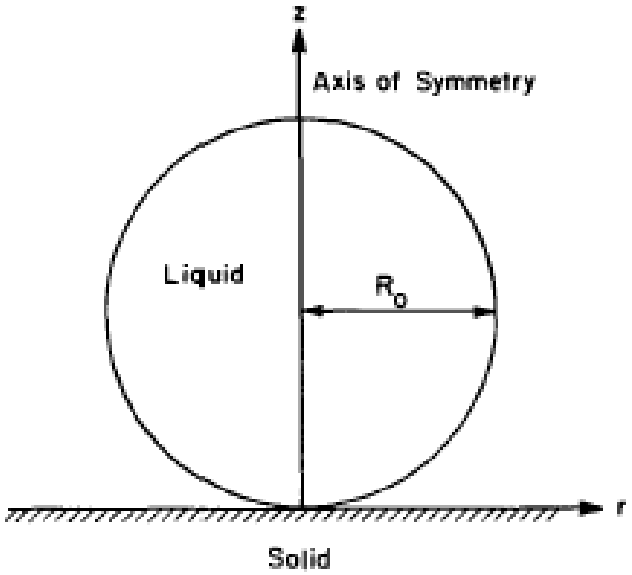


**Fig. 1—The problem domain and the coordinate systems.**

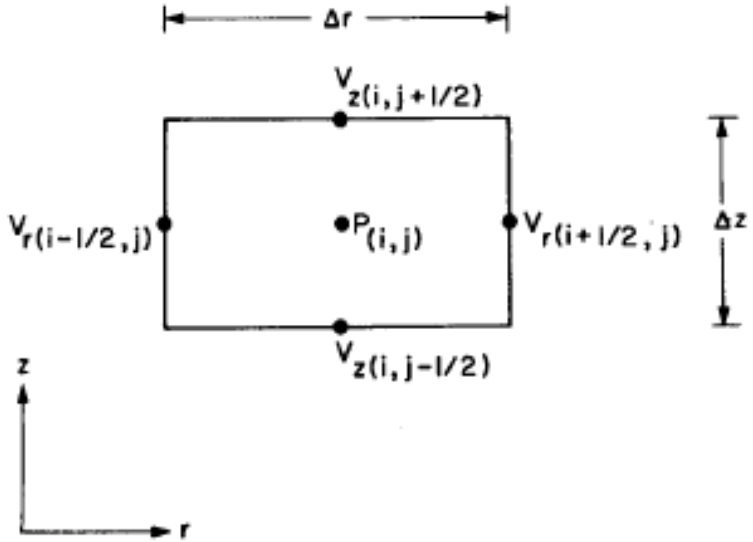


**Fig. 2—Locations of velocities and pressure in a MAC cell.**

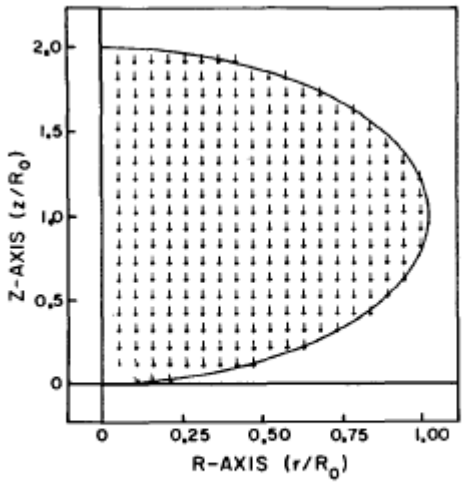


Fig. 3—The velocity distribution at nondimensional time 0.002 (real time 0.4 $\mu$sec). The scales of $R$ and $Z$ axes are normalized with respect to the radius of the drop ($R_o$). The nondimensional velocities (as referenced to the impact velocity, $V_o$) near the solid surface ($Z = 0.025$) are: 0.26, 0.52, 1.26, and 1.09, respectively.

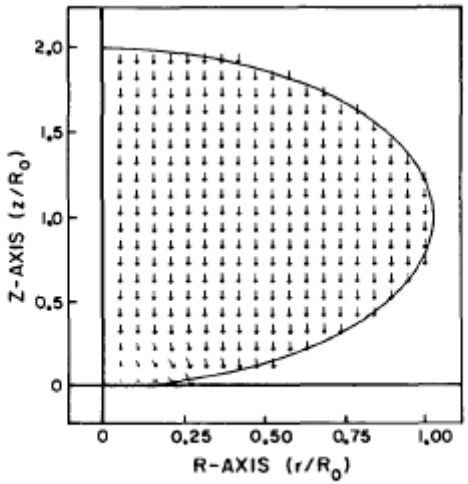


Fig. 4—The velocity distribution at nondimensional time 0.004 (real time 0.8 $\mu$sec). The nondimensional velocities near the solid surface ($Z = 0.025$) are: 0.19, 0.38, 0.60, 1.09, and 1.56, respectively.

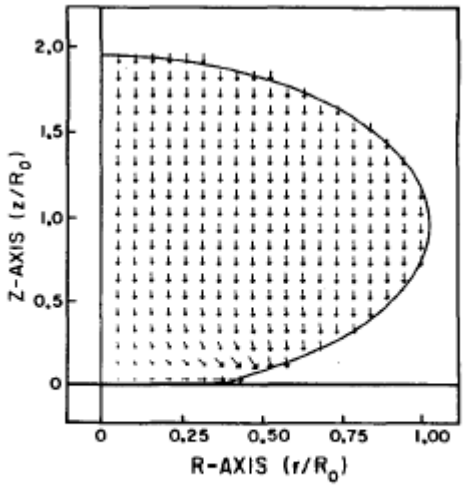


Fig. 5—The velocity distribution at nondimensional time 0.024 (real time 4.8 $\mu$sec). The nondimensional velocities near the solid surface ($Z = 0.025$) are: 0.13, 0.27, 0.41, 0.55, 0.74, 0.92, 1.26, and 1.59, respectively.

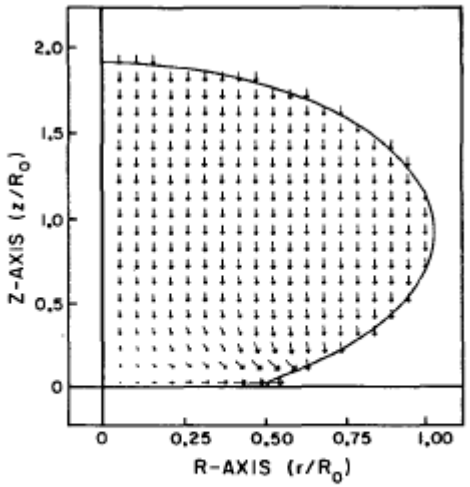


Fig. 6—The velocity distribution at nondimensional time 0.053 (real time 10.6 $\mu$sec). The nondimensional velocities near the solid surface ($Z = 0.025$) are: 0.11, 0.22, 0.34, 0.46, 0.60, 0.74, 1.01, 1.29, 1.68, and 2.01, respectively.

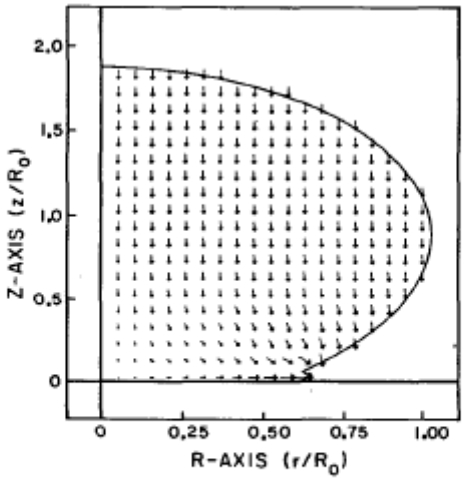


Fig. 7—The velocity distribution at nondimensional time 0.089 (real time 17.8 $\mu$sec). The nondimensional velocities near the solid surface ($Z = 0.025$) are: 0.08, 0.17, 0.25, 0.34, 0.42, 0.50, 0.68, 0.86, 1.15, 1.44, 1.66, and 1.88, respectively.

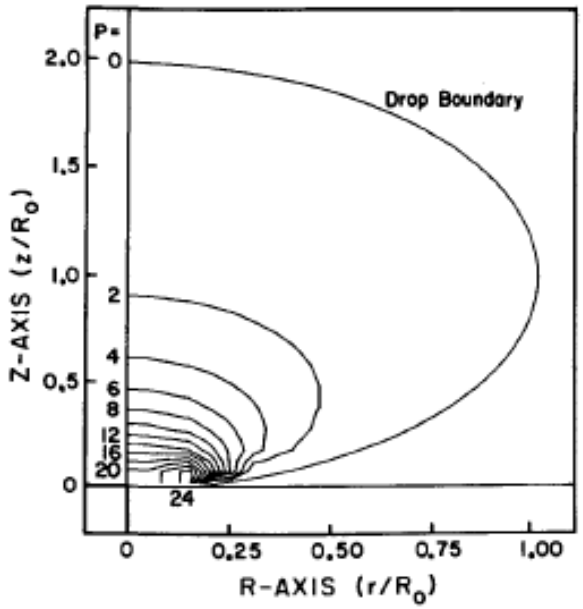


Fig. 8—The isobars within the drop at nondimensional time 0.004 (real time 0.8 μsec). The pressure is normalized with respect to the steady-state stagnation pressure (50 kPa).

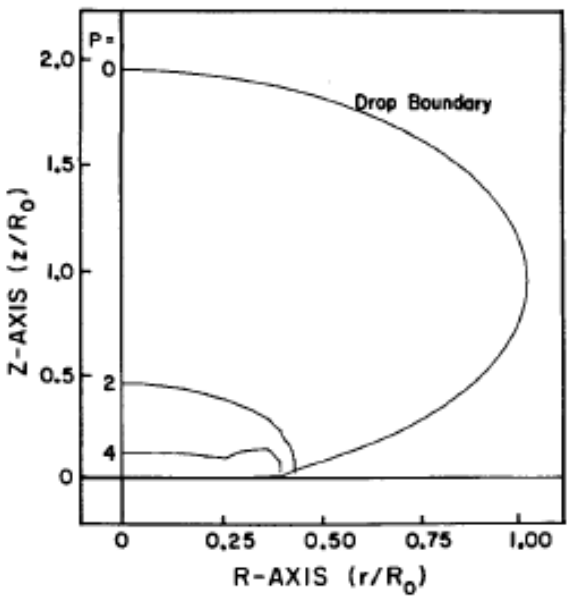


Fig. 9—The isobars within the drop at nondimensional time 0.024 (real time 4.8 μsec).

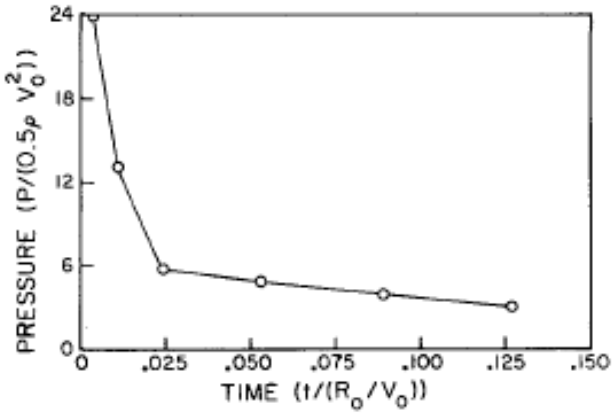


Fig. 10—The maximum pressures vs. time after impact, both in nondimensional scales.

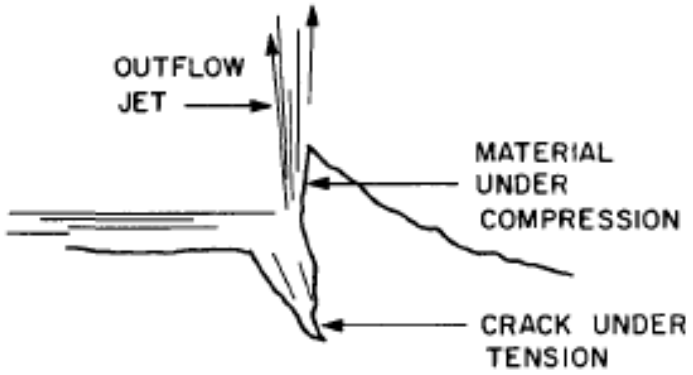


Fig. 11—The effect of lateral jetting on the surface irregularities.

# Raindrop impact phenomena: The elastic deformation case

"A forma como a superfície do solo deforma sob o impacto da gota de chuva determina o ângulo de incidência entre o jato lateral de água e o solo e, subseqüentemente, a quantidade de desprendimento"

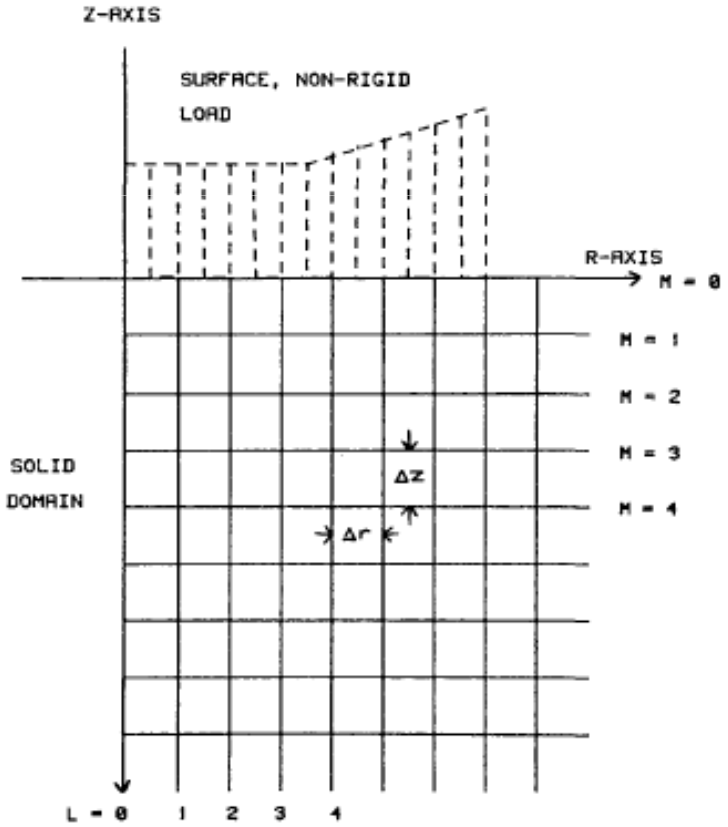


Fig. 1—The solid calculation domain and its discretization.

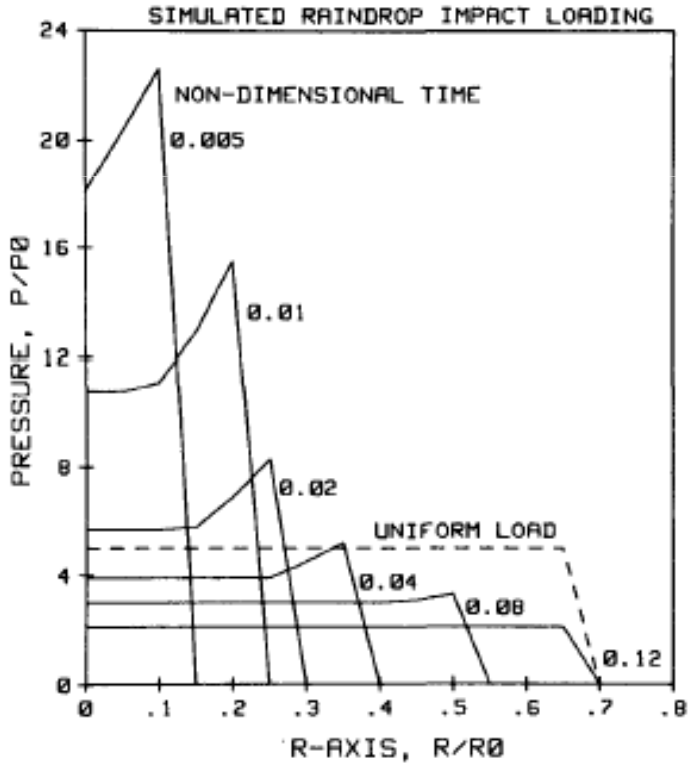


Fig. 2—The simulated load applied on the solid surface at nondimensional time 0.005, 0.01, 0.02, 0.04, 0.08, and 0.12. The dashline shows the steady, uniform load of magnitude 5 $P_o$.

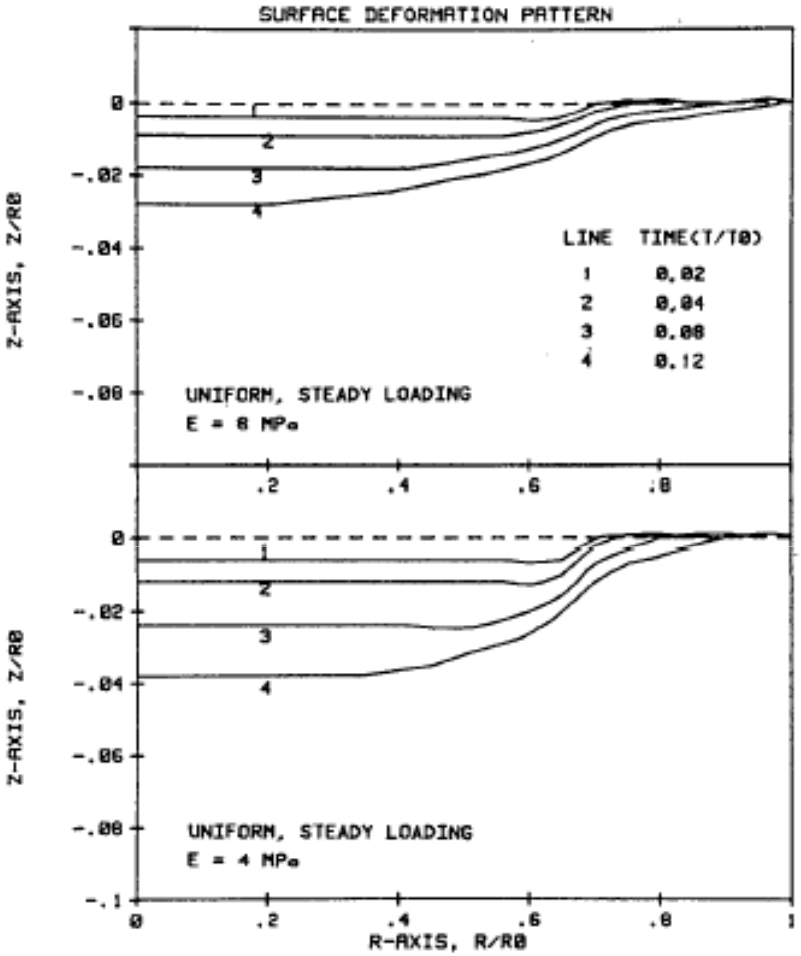


Fig. 3—The surface deformation pattern under steady, uniform load at different time instances after impact. The Young's moduli are 8 and 4 MPa.

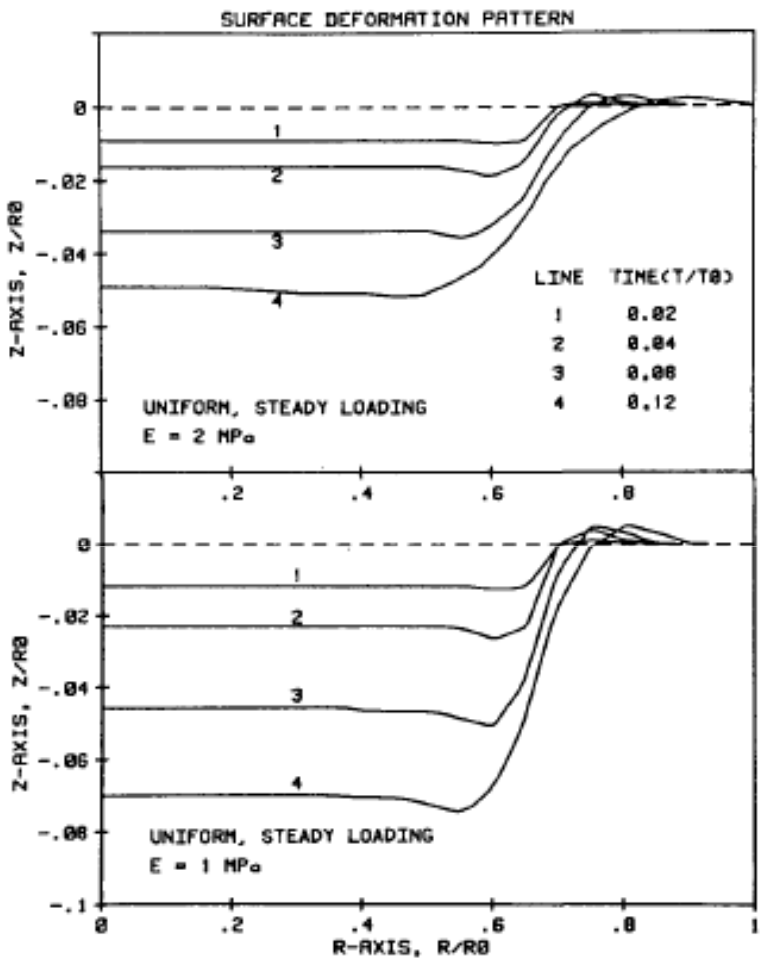


Fig. 4—The surface deformation pattern under steady, uniform load at different time instances after impact. The Young's moduli are 2 and 1 MPa.

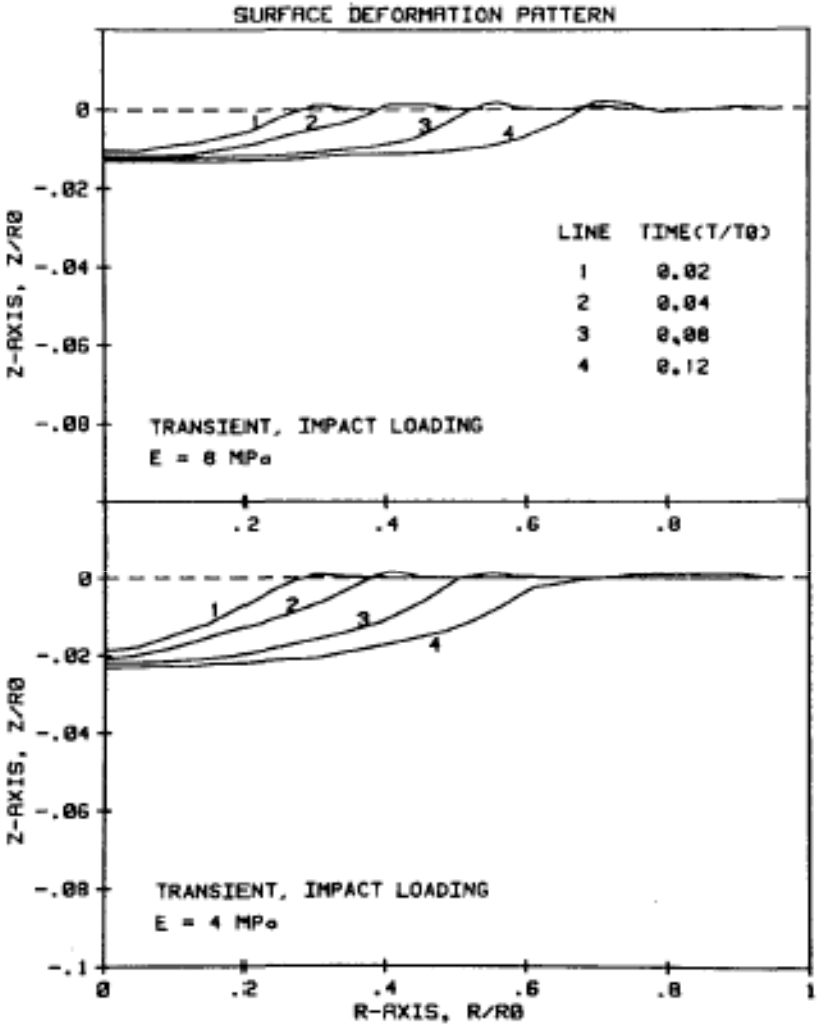


Fig. 5—The surface deformation pattern under simulated raindrop impact load at different time instances after impact. The Young's moduli are 8 and 4 MPa.

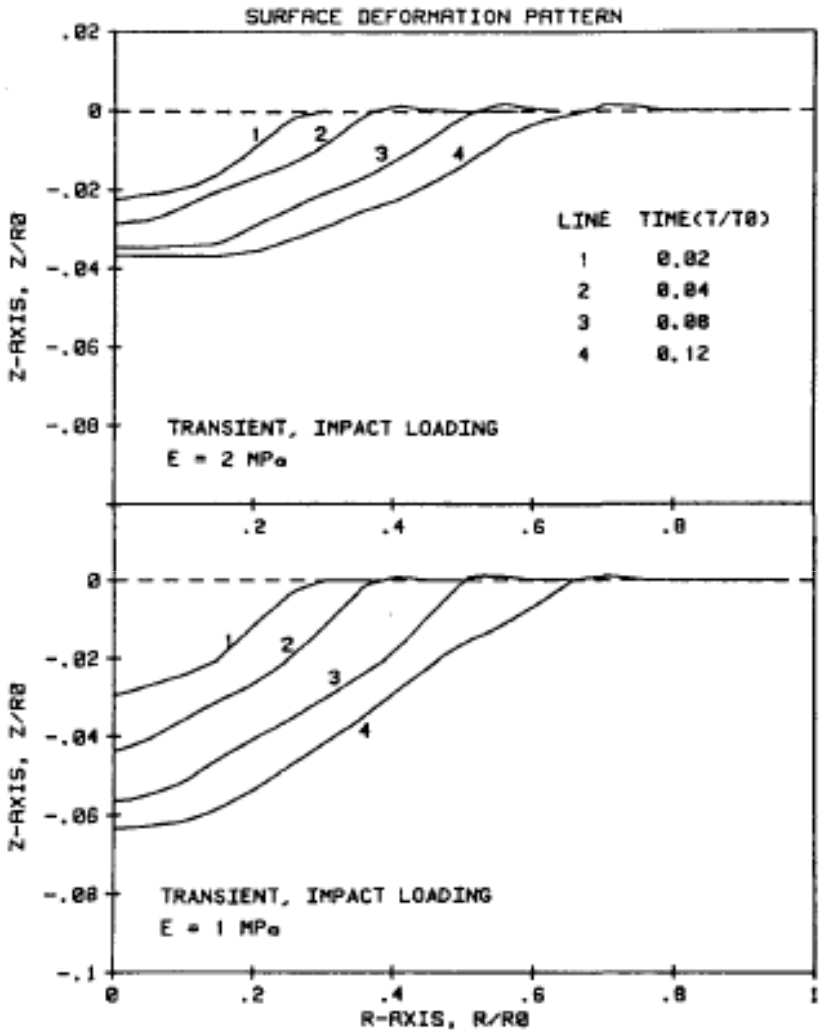


Fig. 6—The surface deformation pattern under simulated raindrop impact load at different time instances after impact. The Young's moduli are 2 and 1 MPa.

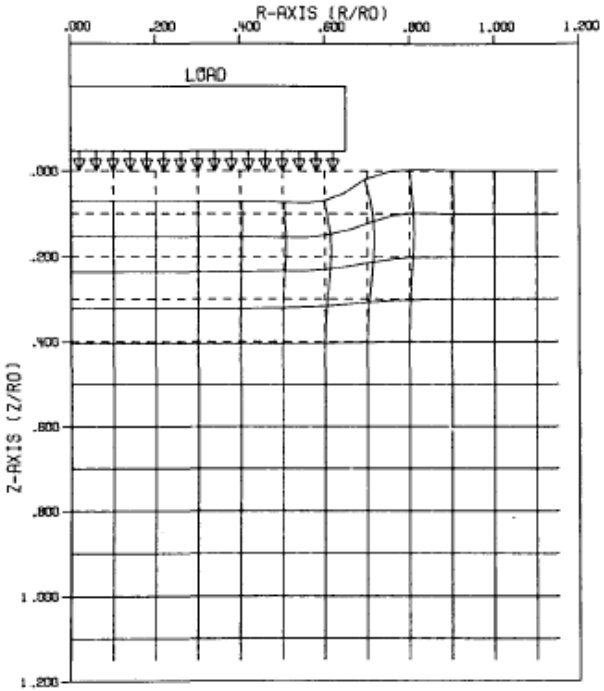


**Fig. 7—The deformation pattern within the solid domain under steady, uniform load. The Young's modulus is 1 MPa and the nondimensional time is 0.12.**

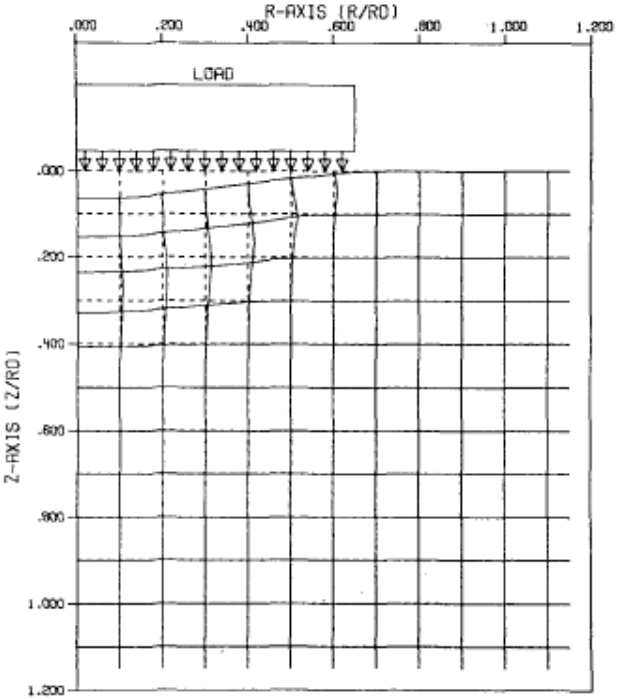


**Fig. 8—The deformation pattern within the solid domain under simulated raindrop impact load. The Young's modulus is 1 MPa and the nondimensional time scale is 0.12.**

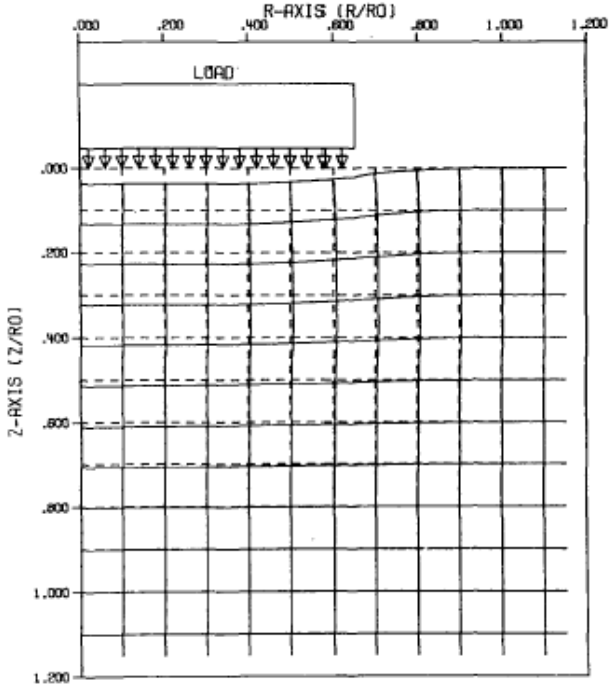


**Fig. 9—The deformation pattern within the solid domain under steady, uniform load. The Young's modulus is 4 MPa and the nondimensional time scale is 0.12.**

# The Mechanism of Raindrop Splash on Soil Surfaces

Uso de fotografia de alta velocidade para fotografar salpicamento de gotas de chuva impactando vários solos com potenciais matriciais, densidade e força de cisalhamento diferentes

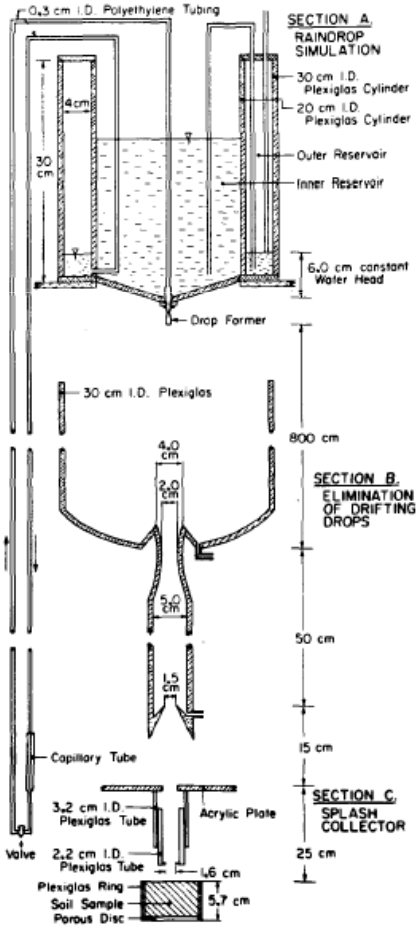


Fig. 1—Schematic diagram of the raindrop tower.

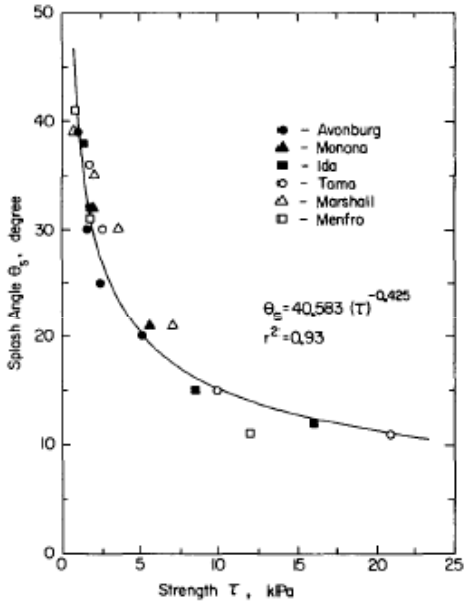


Fig. 1—The relationship between splash angle and soil shear strength.

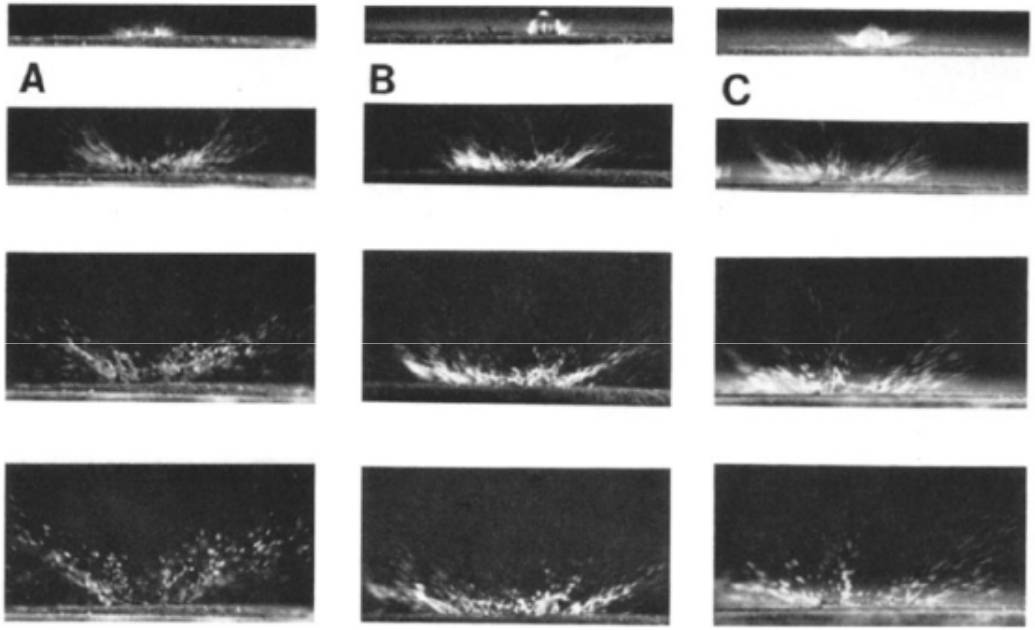


Fig. 2—A series of photographs of splash from Tama silty clay loam at three shear strength levels: (A) $\tau$ = 2.6 kPa; (B) $\tau$ = 7.1 kPa; and (C) $\tau$ = 20.9 kPa.

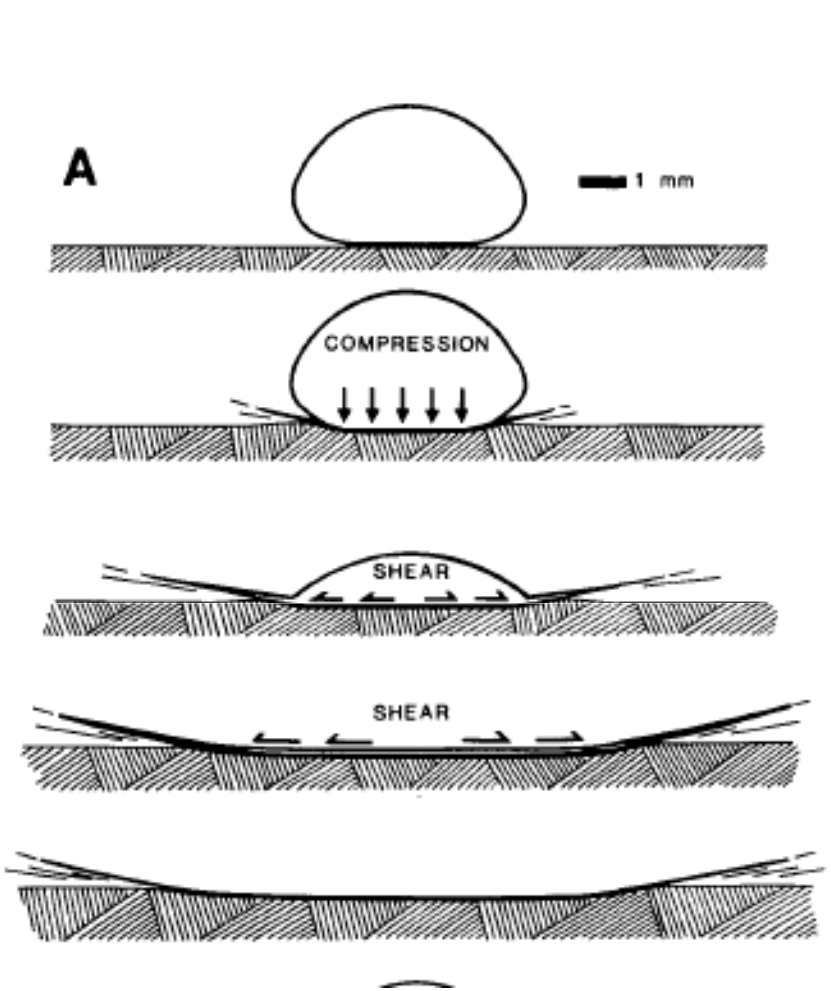


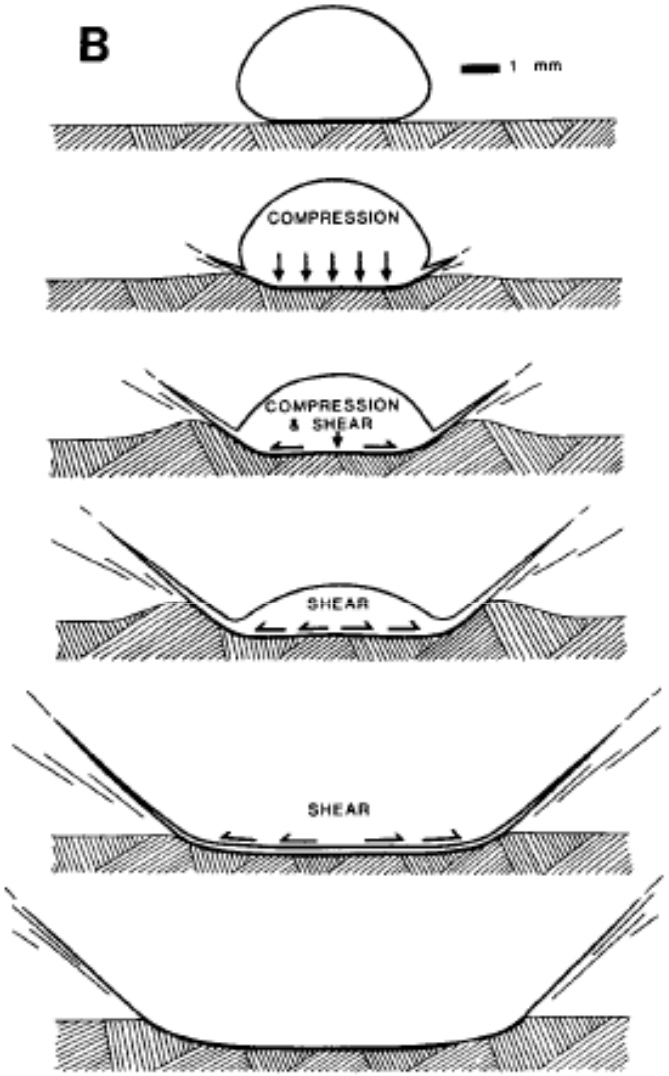


**Fig. 3—Schematic diagram of the splash mechanism at (A) high- and (B) low-strength levels.**

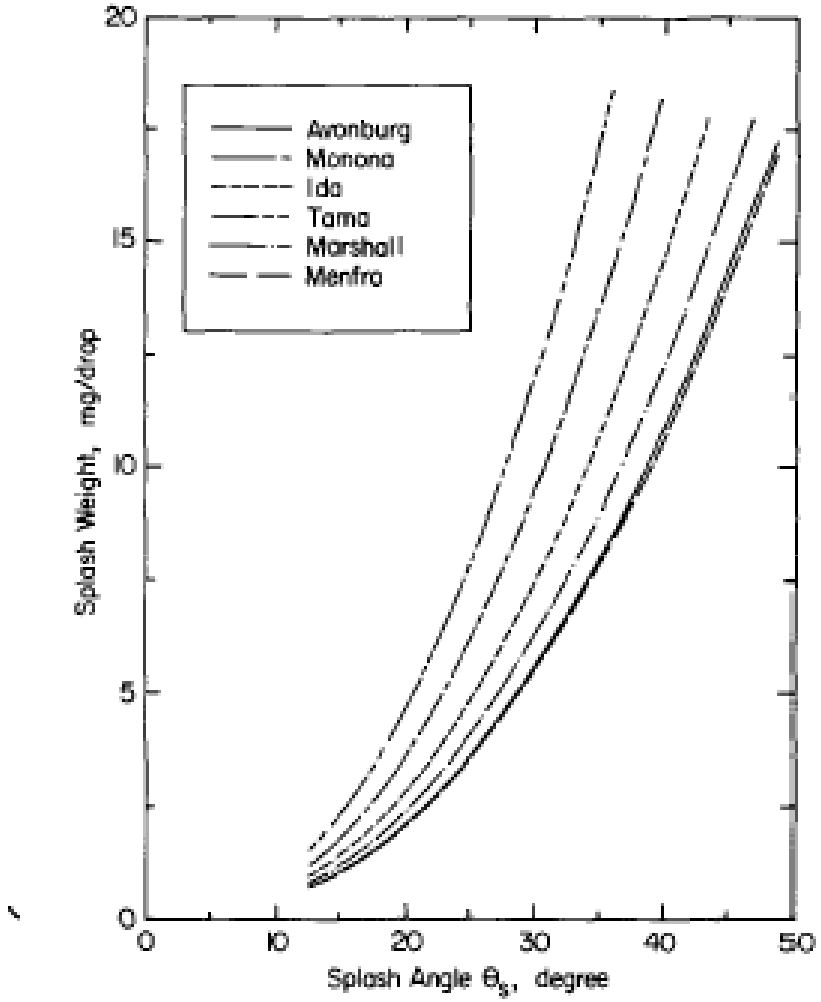


**Fig. 4—The relationship between splash weight and splash angle.**

# Measurement of waterdrop impact pressures on soil surfaces

Utilizando transdutores de pressão e o simulador de gotas anteriormente descrito foi medida a pressão de impacto sobre dois solos com diferentes atributos.

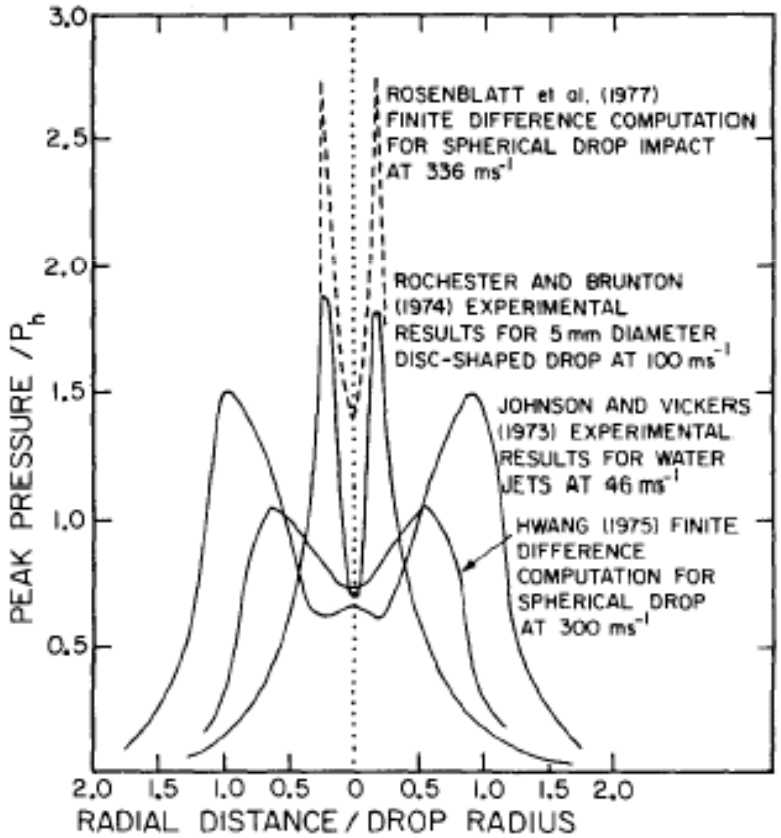


**Fig. 1. Results of peak water impact pressures on rigid surfaces from past studies (from Adler, 1979).**

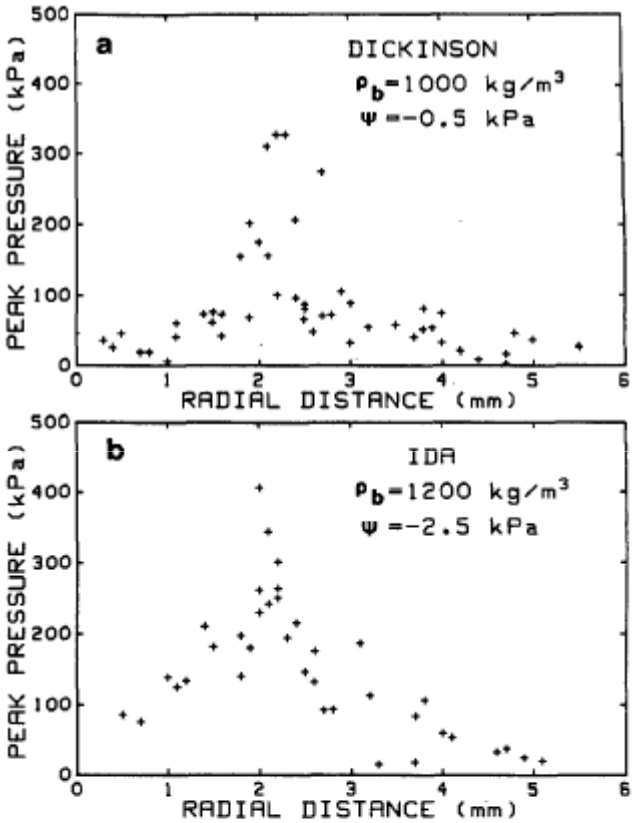


**Fig. 2. Peak pressures vs. radial distance from the center of impact (a) for the Dickinson soil at $\rho_b$ = 1.0 Mg/m$^3$ and Ψ = −0.5 kPa, and (b) for the Ida soil at $\rho_b$ = 1.2 Mg/m$^3$ and Ψ = −2.5 kPa.**

**Table 1. Peak pressures of impact on soil surfaces for a 5.6-mm diam drop falling from 14 m.**

| Soil type | Bulk density | Matric potential | Distance from crater center | Mean peak pressure | SD | No. of impacts |
|---|---|---|---|---|---|---|
| | Mg/m$^3$ | kPa | mm | kPa | | |
| Dickinson | 1.0 | −0.5 | 0.0–1.7 | 44 | 22 | 14 |
| | | | 1.8–2.3 | 201 | 98 | 9 |
| | | | 2.4–6.0 | 66 | 56 | 28 |
| | | −2.5 | 0.0–1.7 | 91 | 75 | 16 |
| | | | 1.8–2.3 | 209 | 82 | 8 |
| | | | 2.4–6.0 | 78 | 74 | 25 |
| | 1.2 | −0.5 | 0.0–1.7 | 79 | 44 | 14 |
| | | | 1.8–2.3 | 209 | 102 | 10 |
| | | | 2.4–6.0 | 59 | 59 | 15 |
| | | −2.5 | 0.0–1.7 | 83 | 38 | 13 |
| | | | 1.8–2.3 | 249 | 70 | 8 |
| | | | 2.4–6.0 | 77 | 70 | 18 |
| Ida | 1.0 | −0.5 | 0.0–1.7 | 98 | 51 | 9 |
| | | | 1.8–2.3 | 200 | 86 | 7 |
| | | | 2.4–6.0 | 69 | 56 | 26 |
| | | −2.5 | 0.0–1.7 | 97 | 47 | 9 |
| | | | 1.8–2.3 | 190 | 58 | 11 |
| | | | 2.4–6.0 | 57 | 52 | 28 |
| | 1.2 | −0.5 | 0.0–1.7 | 113 | 52 | 9 |
| | | | 1.8–2.3 | 289 | 168 | 8 |
| | | | 2.4–6.0 | 68 | 48 | 33 |
| | | −2.5 | 0.0–1.7 | 135 | 48 | 7 |
| | | | 1.8–2.3 | 250 | 74 | 12 |
| | | | 2.4–6.0 | 91 | 63 | 18 |